Title

Erratum to “Distributed energy storage system scheduling considering tariff structure, energy arbitrage and solar PV penetration” [Appl. Energy 205 (2017) 1384–1393]

Authors

Babacan, Oytun
Ratnam, Elizabeth L
Disfani, Vahid R
et al.

Publication Date

2018-06-01

DOI

10.1016/j.apenergy.2017.12.079

Peer reviewed

Distributed energy storage system scheduling considering tariff structure, energy arbitrage and solar PV penetration

Oytun Babacan[a,*], Elizabeth L. Ratnam[b], Vahid R. Disfani[a], Jan Kleissl[a]

[a] *Department of Mechanical and Aerospace Engineering, University of California San Diego, La Jolla, CA, 92093 USA*
[b] *Berkeley Energy & Climate Institute, University of California Berkeley, Berkeley, CA 94720*

Abstract

We develop a new convex optimization (CO)-based charge/discharge scheduling algorithm for distributed energy storage systems (ESSs) co-located with solar photovoltaic (PV) systems. The CO-based scheduling algorithm minimizes the monthly electricity expenses of a customer who owns an ESS and incorporates both a time-of-use volumetric tariff and a demand charge tariff. Further, we propose the novel idea of a "supply charge" tariff that incentivizes ESS customers to store excess solar PV generation that may otherwise result in reverse power flow in the distribution grid. By means of a case study we observe the CO-based daily charge/discharge schedules reduce (1) peak net demand (that is, load minus PV generation) of the customer, (2) power fluctuations in the customer net demand profile, and (3) the reliance of the customer on the grid by way of promoting energy self-consumption of local solar PV generation. Two alternate methods for behind-the-meter ESS scheduling are considered as benchmarks for cost minimization, peak net demand reduction, and mitigation of net demand fluctuations. The algorithm is tested using real 30-minute interval residential load and solar data of 53 customers over 2-years. Results show that the CO-based scheduling algorithm provides mean peak net demand reductions between 46% - 64%, reduces mean net demand fluctuations by 25% - 49%, and increases the mean solar PV self-consumption between 24% - 39% when compared to a customer without an ESS. Introduction of a supply charge reduces the maximum solar PV power supply to the grid by 19% on average and does not financially impact ESS owners.

Keywords: Energy storage, Solar PV, Time-of-use tariff, Demand charge, Reverse power flow, Peak-load reduction

1. Introduction

Energy storage systems (ESS) are regarded as an enabling element of a future low-carbon electric grid as they allow higher amounts of renewable energy on the grid (de Sisternes et al., 2016; DiOrio et al., 2015). This stems, in part, from the operational flexibility ESS offer grid operators facilitating the integration of intermittent wind and solar power (Denholm et al., 2010). Increasing penetration of solar PV on the electric grid requires a new planning paradigm for capacity resources, which have traditionally been procured to meet system peak load and reserve requirements. Now, additional capacity is needed to provide flexible generation for integrating variable generation as well (Cutter et al., 2014). The proliferation of distributed ESS could provide this needed flexibility for a transforming grid.

With the rapid growth in grid-connected solar PV, electric utilities are facing stagnant electricity sales, particularly in the residential sector. This reduction in sales reduces the utility's ability to recover capital costs, which constitutes the majority of their expenses (McLaren et al., 2015). At the same time, the PV system owners still rely on the grid for voltage and frequency control and for their night-time demand. They also need the grid to receive the economic benefit from exporting excess generation. However, as solar PV penetration in a distribution system increases, power flow direc-

*Corresponding Author
Email addresses: obabacan@ucsd.edu (Oytun Babacan), eratnam@berkeley.edu (Elizabeth L. Ratnam), disfani@ucsd.edu (Vahid R. Disfani), jkleissl@ucsd.edu (Jan Kleissl)

tion can reverse, potentially causing power quality, protection, and reliability issues due to local and intermittent electricity generation during daytime (Baran et al., 2012).

Electric utilities might have difficulties addressing these problems without raising electricity rates. Instead, the ESS owners could be incentivized to support the electric grid through time-of-use tariffs and/or residential demand charges. Through demand charges the ESS owners have the opportunity to reduce their electricity bills by managing their demand and they also gain access to reduced volumetric electricity rates. Customer participation in demand charge tariffs benefits electric utilities since demand charges, in theory, reduce the need for new infrastructure investment and overall system costs. (Hledik, 2014).

There is an extensive literature on ESS charge/discharge scheduling for residential buildings that are coupled with a solar PV system. Several of these, e.g. (Luthander et al., 2016; Moshövel et al., 2015; Ren et al., 2016a), focus on increasing the consumption of solar PV generation locally and mitigating the peak power flows from and to the grid. However, they do not consider a demand charge tariff.

There are also a number of studies that consider a demand charge in their scheduling formulation. Geem and Yoon (2017) propose a population-based heuristic algorithm that reduces peak net demand of the customer and on-peak electricity purchases. Zheng et al. (2015) introduce a scheduling algorithm to reduce peak net demand and evaluates the economical feasibility of different energy storage technologies. Gitizadeh and Fakharzadegan (2014) formulate a Mixed Integer Linear Program (MILP) problem to optimize the capacity of ESS for peak net demand reduction and energy shifting.

However, these studies fall short of demonstrating a stand-alone scheduling algorithm for charging and discharging ESS. More specifically, Zheng et al. (2015) and Gitizadeh and Fakharzadegan (2014) use a scheduling algorithm as a representative tool to investigate another research question, and Geem and Yoon (2017) do not present a comprehensive validation study of the algorithm. Moreover, to date, there is no modeling framework for energy storage scheduling that incorporates both a time-of-use tariff and a demand charge tariff while dynamically adjusting a monthly peak demand prediction for the customer.

In this context, the modeling framework proposed in this paper includes a novel convex optimization (CO)-based scheduling algorithm for distributed customer-sited ESSs (Section 2) and a novel supply charge option in electricity rate offerings.

The objective of the algorithm is to provide financial benefit to the ESS owner while inherently (1) reducing the peak net demand of the customer, (2) mitigating power fluctuations in the customer net demand profile, and (3) increasing local PV generation consumption for a co-located solar PV system. The ESS specifications, day-ahead load and solar forecast and the electric tariff are sufficient to deploy the algorithm on site. By means of a case study we benchmark the ability of the algorithm to minimize cost, reduce peak net demand, and mitigate net demand fluctuations, and compare it against two alternate methods proposed in the literature (Section 3 - 4).

A supply charge provides an incentive to customers to either self-consume PV generation, or to curtail their generation output when it exceeds their load requirements, thereby reducing the reverse power flow in the distribution grid. We discuss its impact on the grid, on the ESS cycling, and on the customer bill by comparing it against a demand charge only case (Section 4). Section 5 concludes the paper.

2. Problem Formulation

2.1. Notation

Herein $\mathbb{R}^s$ denotes s-dimensional vectors of real numbers, where $\mathbb{R}^1 = \mathbb{R}$ and $\mathbb{1} \in \mathbb{R}^{s\geq 0}$ denotes the all-1 s column vector of length s. $s = 24\text{h}/\Delta t$ is the number of time steps in a day-long charging schedule, where Δt is the time-interval between consecutive time-steps k in hours. $\mathbf{I}$ denotes the identity matrix of size s and $\mathbf{T} = [t_{ij}]$ denotes the s-by-s matrix satisfying $t_{ij} = 1$ for $i \geq j$ and $t_{ij} = 0$ elsewhere. We denote vectors in bold and represent matrices using uppercase bold characters.

2.2. Customer System Configurations

We model four system configurations shown in Figure 1 for customer-owned, grid-connected ESS, which might represent, for example, a residential household or a commercial business. Configurations a and b consist of an ESS and a customer load without PV. Configuration a prohibits the customer from selling electricity to the grid, whereas

configuration b compensates the customer at the retail rate for delivering energy to the grid, thus allows energy arbitrage opportunities. Configurations c and d incorporate a customer-owned, grid-connected solar PV system into the configurations a and b, respectively. We assume customers with configuration c curtail solar PV generation when their energy storage is full and the solar PV system generation exceeds load, i.e. when net demand is negative.

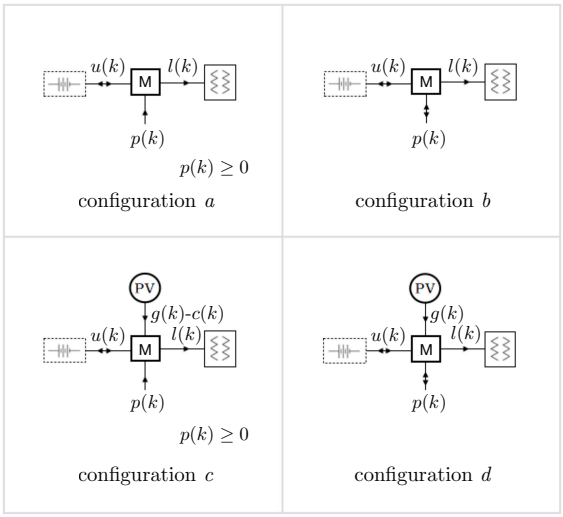

Figure 1: Configurations of the customer system under consideration. M represents the electricity meter of the customer. The average net demand over a period Δt is denoted $p(k)$ with k being the time step index, and is positive when flowing from the grid to the customer. The average ESS charge/discharge over Δt is denoted $u(k)$, and is positive when discharging. The average load of the system over Δt is $l(k)$. The average generated and curtailed power from the solar PV system over Δt is $g(k)$ and $c(k)$, respectively.

For each system configuration, the power balance equation for the net demand $p(k)$ is given by

$$p(k) = l(k) - g(k) + c(k) - u(k) \tag{1}$$

for all time step indices $k \in \{1, ..., s\}$. All units are in kW. The average load of the system over a period Δt is $l(k)$, the average solar PV generation is $g(k)$, the average curtailed solar PV generation is $c(k)$, and the average ESS charge/discharge is $u(k)$, where $c(k)$ is zero for all time steps $k \in \{1, ..., s\}$ in configurations a, b and d, and $p(k)$ is nonnegative for all time steps $k \in \{1, ..., s\}$ in configurations a and c.

The constraint $p(k) \geq 0$ depicts the scenario where there is no financial incentive for energy to be sold to the grid. That is, in such cases curtailed solar generation $c(k)$ is equivalent to the excess PV generation that would have ordinarily been injected into the grid but this supply would not result in financial compensation to the customer.

2.3. Regulation and Accounting

A customer is billed monthly based on kWh electricity consumption via a *time-of-use* (TOU) tariff denoted by the length-s vector $\mathbf{\Lambda}_\mathrm{e} \in \mathbb{R}^s$. In addition, a net-metering program is considered in configurations b and d, in which a customer receives compensation for exported electricity at a rate equivalent to the TOU tariff.

We use two additional tariff mechanisms: A *demand charge* denoted by the scalar Λ_d, and a *supply charge* denoted by the scalar Λ_s which is a new concept to regulate reverse power flows. A demand charge prevents the customers from simply shifting their on-peak demand to an off-peak period without reducing their peak demand and encourages the customer to reduce their peak demand regardless of the TOU pricing period.

A supply charge addresses the problem of excessive electricity sales to the grid especially during solar peak hours. This rule provides an incentive to the customers to either self-consume PV generation, or to curtail their generation output when it exceeds their load requirements. The supply charge is a new concept motivated by PV export being limited to a fixed fraction of PV capacity in some markets (e.g. Germany), but provides an economic incentive to reduce exports rather than a strict rule. In what follows a *capacity charge* (CC) combines both a demand charge and supply charge.

Without loss of generality, we assume here the supply charge tariff is equal to the demand charge tariff. Then, the customer monthly peak net demand is subject to the CC tariff $\Lambda = \Lambda_\mathrm{s} = \Lambda_\mathrm{d}$. The CC is based on the peak electricity supplied to the customer or delivered to the grid across a month. That is, the customer's largest absolute net demand over each month is multiplied by the CC tariff Λ in the billing process.

2.4. Energy Storage System Model

We constrain the ESS charge/discharge $u(k)$ by $\underline{B} \leq u(k) \leq \overline{B}$, where $\underline{B}$ and $\overline{B}$ are the discharge and charge power limit of the ESS, respectively.

The state of charge (SOC) is defined by

$$\chi(k) := \chi(0) - \sum_{k=1}^{s} u(k)\Delta t, \tag{2}$$

where $\chi(0)$ denotes the initial state of charge.

The rated energy capacity of the ESS is represented by C in kWh. We represent the *minimum allowed SOC* and the *maximum allowed SOC* of the ESS in kWh as $\underline{\chi}$ and $\overline{\chi}$, where $\underline{\chi} := 0$ and $\overline{\chi} := C$. Note that $\underline{\chi}$ could be set to a fraction of C for a specific energy storage technology that would otherwise degrade when fully discharged. It is assumed here that the efficiency of the ESS is 100% and that degradation is negligible. Hence we model the upper limit of performance for a technology neutral ESS. That is, the ESS model is deliberately simplified to encompass a range of different ESS technologies. For specific applications, this idealized model could be replaced with a more complex representation of a specific energy storage technology.

In simulation, we assume each customer has an ESS with an identical storage capacity of 10 kWh and a charging and discharging limit of 5 kW. This is centered within the range of ESS capacities (2-22kWh) considered in other residential ESS studies (Luthander et al., 2016; Ranaweera and Midtgård, 2016; Ratnam et al., 2015a; Ren et al., 2016a,b; Vieira et al., 2017; Zhang et al., 2016). Customer load and PV generation characteristics are provided in Section 3.2.

2.5. Scheduling Algorithm

We construct a constrained optimization problem to minimize the monthly electricity bill of a customer with an ESS. The customer-owned ESS is dispatched daily solving the following convex optimization problem:

$$\min_{\boldsymbol{p}\in\mathbb{R}^s} \Delta t \boldsymbol{\Lambda}_{\mathrm{e}}^T \boldsymbol{p} + \Lambda[\max\{||\boldsymbol{p}||_\infty, p^*\} - p^*], \tag{3}$$

such that $\boldsymbol{A}\boldsymbol{u} \leq \boldsymbol{b}$, $\mathbb{1}^T\boldsymbol{p} = 0$, where $\boldsymbol{A} \in \mathbb{R}^{4s\times s}$, $\boldsymbol{b} \in \mathbb{R}^{4s}$, $\boldsymbol{u} \in \mathbb{R}^s$, $\boldsymbol{\Lambda_e} \in \mathbb{R}^s$, $\Lambda \in \mathbb{R}$, $p^* \in \mathbb{R}$. The customer net demand $\boldsymbol{p}$ is defined by Eq. 1, where $\boldsymbol{l} \in \mathbb{R}^s$, $\boldsymbol{g} \in \mathbb{R}^s$, $\boldsymbol{c} \in \mathbb{R}^s$, and $k \in \{1, ..., s\}$. For configurations a and c, $\boldsymbol{p} \geq 0$. The infinity-norm of $\boldsymbol{p}$ is $||\boldsymbol{p}||_\infty = \max\limits_{1\leq k\leq s} |p_k|$. The first term of Eq. 3 accounts for the time-of-use electricity costs, and the the second term of Eq. 3. accounts for the demand charges.

The objective function defined by Eq. 3 is constrained by the ESS charge and discharge limits, capacity constraints, the state of charge dynamics defined in Eq. 2, and by a final state of charge limit. In more detail, the inequality constraint $\boldsymbol{A}\boldsymbol{u} \leq \boldsymbol{b}$ captures the ESS dynamics defined by Eq. 2 together with the minimum and maximum SOC allowed ($\overline{\chi}$ and $\underline{\chi}$), in addition to the charge and discharge power limits ($\overline{B}$ and $\underline{B}$), where $\boldsymbol{A} = \begin{bmatrix} \boldsymbol{I} & -\boldsymbol{I} & \boldsymbol{T} & -\boldsymbol{T} \end{bmatrix}^T \in \mathbb{R}^{4s\times s}$, $\boldsymbol{b} = \begin{bmatrix} \overline{B}\mathbb{1}^T & \underline{B}\mathbb{1}^T & \underline{C}\mathbb{1}^T & \overline{C}\mathbb{1}^T \end{bmatrix}^T \in \mathbb{R}^{4s}$ and $\boldsymbol{u}$ is the ESS charge/discharge rate. Each component of the ESS model was introduced in Section 2.1 and 2.4. Note that the derivation of $\overline{C}$ and $\underline{C}$ is straightforward, and is given in Ratnam et al. (2015a).

The equality constraint $\mathbb{1}^T\boldsymbol{p} = 0$ prevents energy-shifting between days. It ensures that $\chi(s)$, the final SOC at time $s\Delta t$, equals to the initial SOC $\chi(0)$ and hence prevents the ESS from storing extra energy for the following day. Throughout the simulations we set $\chi(0)$ to 50% of the rated energy capacity C, that is also consistent with the approach taken in Ratnam et al. (2015a).

If $||\boldsymbol{p}||_\infty \leq p^*$, then the formulation in Eq. 3 is equivalent to the minimization of the linear objective function $\Delta t\boldsymbol{\Lambda}_{\mathrm{e}}^T\boldsymbol{p}$ with the inequality constraint $||\boldsymbol{p}||_\infty \leq p^*$. Otherwise $||\boldsymbol{p}||_\infty$ replaces the existing p^* as the new net demand prediction for the days remaining in the billing period. Thus, this formulation does not require any integer value in the constraints.

Since there is no cost associated with the charge/discharge rate or excessive cycling of the ESS in the objective function, the CO-based scheduling algorithm might charge or discharge the ESS within the same TOU pricing period without any financial benefit to the customer. To eliminate these instances we add a penalty term f_{penalty} to Eq. 3 given by

$$f_{\mathrm{penalty}} = 10^{-6}||\boldsymbol{u}||_2 \ , \tag{4}$$

where $||\boldsymbol{u}||_2 \in \mathbb{R}^s$ is the Euclidean norm of the ESS charge/discharge schedule. We multiply the Euclidean norm with 10^{-6}\$/kW to make it small compared to the rest of the objective function in Eq. 3 ensuring it does not alter the minimum objective function value achieved.

We solve the CO-based scheduling algorithm using MATLAB (Version 2016b) with the convex modeling framework CVX (Version 2.1) and the solver Gurobi (Version 7.0.2).

2.6. Operational Inputs

At the start of each day, a day-ahead forecast for solar PV generation and a day-ahead load prediction are required for each customer. Since demand and solar forecast techniques are not within the focus of this study, the day-ahead forecasts are taken equal to the observed data, i.e. perfect information. While it is not realistic to assume availability of such forecasts, with this perfect information we model the upper limit of performance of the CO-based scheduling algorithm. That is, forecast errors typically result in increased demand charges due to premature ESS discharges.

In addition, at the beginning of each month a prediction, p^*, is made for the month-ahead customer absolute net demand peak to avoid excessive peak reductions during the first days of the month. The CO-based scheduling algorithm is used to find the optimal dispatch solution of the ESS for the month-long ($N_{\text{day}} \times s$) data set collected during the previous month. The resulting maximum absolute net demand is used as the prediction, p^*, for the current month.

Net demand prediction is an essential component for economic performance of the CO-based scheduling algorithm but if a simpler implementation was desired, p^* could be set to zero at the beginning of the month.

2.7. Customer Billing

The billing period spans a calendar month starting with the first day of each month of the year. The TOU (volumetric) electricity charges, denoted by (EC), for a calendar month are defined by

$$\text{EC} := \sum_{n=1}^{N_{\text{day}}} \Delta t \boldsymbol{\Lambda}_{\text{e}}^T \boldsymbol{p}_n \,, \tag{5}$$

where N_{day} is the number of days in the month and $\boldsymbol{p}_n$ is a vector of size s representing the daily net demand profile (e.g., the first day of the month $\boldsymbol{p_1} = \{p_{1,1}, ..., p_{1,s}\}$).

Peak capacity charges, denoted by CC, are also factored into the monthly bill and are defined by

$$\text{CC} := \Lambda p_{\max} \,, \tag{6}$$

where $p_{\max} = \max(||\boldsymbol{p}_1||_\infty, ..., ||\boldsymbol{p}_{N_{\text{day}}}||_\infty)$ is the maximum absolute net demand of the customer observed in the calendar month.

The total monthly electricity bill (i.e., total charge), denoted by TC, is then

$$\text{TC} := \text{EC} + \text{CC} \,. \tag{7}$$

3. Performance Metrics, Residential Customer Data, and Tariff

3.1. Performance Metrics

In addition to the reductions in the customer electricity bill defined in Section 2.7, we define metrics to quantify how the charge/discharge schedules affect peak demand, PV self-consumption, the net demand profile, and ESS cycling.

Peak Capacity Reduction is the percentage reduction in a customer's peak capacity in a billing month achieved relative to the original net demand without ESS. Peak capacity is defined as the highest 30-minute kW measurement during a billing month.

PV self-consumption is the total amount of solar generation that is consumed locally during the solar hours normalized by the total amount of solar generation. The customers without an ESS consume PV generation insofar as it coincides with their daytime load. A greater portion of the solar PV generation can be consumed locally by storing generation via an ESS.

Net Demand Fluctuations (NDF) are the sum of the absolute values of differences in adjacent elements of $\boldsymbol{p}$, i.e. fluctuations in the customer net demand profile, normalized by the mean of the absolute net demand, $\overline{||\boldsymbol{p}||}_\infty$.

ESS Cycling is defined as the sum of the absolute values of differences in adjacent elements of $\boldsymbol{u}$, i.e. the number of charge/discharge cycles.

3.2. Customer Load and PV Data

We consider publicly available residential PV generation and load data for customers located in distribution networks operated by Ausgrid, an electricity utility in Australia. The data set includes 3 years of separately reported kWh measurements of load and PV generation, beginning 1 July 2010 with 30-minute averaging intervals.

We use a subset of the originally released data set that contains 54 customers with the highest quality data per Ratnam et al. (2015b). The customer IDs of this subset are given in Table 4 of Ratnam et al. (2015b). We further discard Customer 2 as some data recordings of this customer are missing. The average daily energy consumption among these 53 customers is 17.4 kWh with a minimum of 7.0 kWh and a maximum of 35.4 kWh. The average PV system size is 2.5 kW with a minimum of 1.1 kW and a maximum of 10.0 kW. The average daily PV generation is 9.0 kWh with a minimum of 4.2 kWh and a maximum of 39.3 kWh.

3.3. Tariff

Table 1: Ausgrid Residential TOU tariff (EA025) network energy prices (Ausgrid, 2016). This tariff is effective from 1 July 2016 to 30 June 2017 including goods and services tax in Australia. These energy prices are multiplied with a constant of 0.56 to adjust the original customer electricity bills to the addition of a demand charge to this volumetric energy charge only TOU tariff.

		Energy Prices
Time of Use	Designation	(AU¢/kWh)
Until 7:00	Off-peak	2.7863
7:00 - 14:00	Shoulder	5.4762
14:00 - 20:00	On-Peak	26.4651
20:00 - 22:00	Shoulder	5.4762
Until Midnight	Off-peak	2.7863

We consider the residential TOU tariff EA025 (Ausgrid, 2016) in Table 1. The TOU tariff does not include a demand charge, so we include the demand charge of the TOU tariff EA302 (Ausgrid, 2016), which is approximately 10.7 AU$/kW-month. Hledik (2014) reports that demand charges in the current U.S. tariffs vary between US$1.50/kW-month and US$18.10/kW-month and the EA302 demand charge tariff roughly lies at the mean of this range. The supply charge tariff is set equal to this demand charge tariff.

As we add a demand charge, we subsequently reduce volumetric rates since tariffs with a demand charge often have lower volumetric charges, e.g. Schedule 1S of Virginia Electric & Power Company (VEP, 2016) and TOU-RD-3 of Georgia Power (GP, 2016). To avoid overestimating the bill savings we scale down the volumetric charges of EA025 by a constant such that the average customer bill is the same amount as without a demand charge. By means of iterative computation we determined a constant scale factor of 0.56.

4. Case Studies and Results

Here we introduce six case studies that benchmark the performance of the CO-based scheduling algorithm and examine the effects of introducing a supply charge to the existing tariff structure. These case studies are labeled *case monthly* (*CM*), modified *case monthly* (*CM**), *reference monthly* (*RM*), *reference daily* (*RD*), *linear program* (*LP*), *quadratic program* (*QP*). In what follows each of these case studies is explained in detail. An overview of all case studies is given in Table 2.

4.1. Default case: Case Monthly (CM)

We solve the optimization problem described in Section 2.5 over all days in a billing month individually (as opposed to over the whole month at once, consider further the *RM* below). On the first day of each billing month, a net demand prediction, p^*, for the current month is made as described in Section 2.6. This net demand prediction is updated when it is exceeded by a daily dispatch solution during that month. We denote this case as the *CM* (case monthly).

When the *CM* does not include a supply charge, it is denoted as *CM**. For this case $||\boldsymbol{p}||_\infty$ in Eq. 3 simplifies to $\boldsymbol{p}$ and Λ in Eq. 3 and in Eq. 6 becomes Λ_d.

4.2. Reference Cases

There are two reference cases considered to assess the economic performance of the CO-based scheduling algorithm namely (1) the customer accurately predicts the month-ahead electricity demand and generation, and (2) the customer schedules their ESS without estimating their monthly net demand. These reference cases are structured considering information availability to the customer on historical and future net demand.

RM: Perfect information on monthly net demand

A customer achieves maximum operational savings over a month when TC in Eq. 7 is simultaneously minimized over a set of $\boldsymbol{p}_n$ for all days $n \in \{1, ..., N_\mathrm{day}\}$. In this reference case we optimize with known customer load and solar PV generation of a whole month ($N_\mathrm{day} \times s$).

While it is not realistic to assume knowledge of monthly customer load and solar PV generation, the solution to this reference case determines the theoretical upper bound on TC achievable by the scheduling algorithm. We denote this reference case as *RM* (reference monthly).

RD: Daily Scheduling without p^*

When the daily scheduling solution is determined without a net demand prediction, i.e. $p^* = 0$, the scheduling algorithm overvalues the capacity charge reduction. The resulting scheduling does not necessarily achieve the best economic operation since the daily reduction of the capacity charge is unnecessary when the net demand of a day does not exceed the preexisting maximum net demand.

Table 2: An overview of the case studies. Plus (+) indicates that monthly net demand p^* is predicted for the customer. This prediction is set to 0 for the *RD*. Minus (−) indicates cases that do not consider demand charges in their formulation and thus do not require a net demand prediction. The acronyms of the case studies (Section 4) stand for *case monthly* (*CM*), modified *case monthly* (*CM**), *reference monthly* (*RM*), *reference daily* (*RD*), *linear program* (*LP*), *quadratic program* (*QP*).

Case Study	Method	p^*	Description
CM	CO	+	Default case.
*CM**	CO	+	Default case without considering a supply charge.
RM	CO	+	Best theoretical economic performance achievable by CM.[†]
RD	CO	0	Reference case that minimizes daily (rather than monthly) capacity charge.
LP	LP	-	Best economic performance without a demand or supply charge tariff.
QP	QP	-	Best mitigation of power fluctuations in a net demand profile.

[†]We assume knowledge of month-ahead customer data to construct an upper performance bound for *CM*.

Table 3: The objective functions of the Linear Program (LP) and the Quadratic Program (QP) presented in Ratnam et al. (2015a) along with the CO-based scheduling algorithm presented in this paper. All algorithms have the same set of constraints as described in Section 2.

	CO-based Scheduling Algorithm	Linear Program	Quadratic Program[◇]
Goal	Cost Minimization	Cost Minimization	Power Minimization
Objective Function	$\min_{\boldsymbol{p}\in\mathbb{R}^s} \Delta t \boldsymbol{\Lambda}_{\mathrm{e}}^T \boldsymbol{p} + \Lambda[\max\{\|\|\boldsymbol{p}\|\|_\infty, p^*\} - p^*]$	$\min_{\boldsymbol{p}\in\mathbb{R}^s} \Delta t \boldsymbol{\Lambda}_{\mathrm{e}}^T \boldsymbol{p}$	$\min_{\boldsymbol{p}\in\mathbb{R}^s} \boldsymbol{p}^T \mathbf{I}\, \boldsymbol{p}$

[◇]The matrix $\boldsymbol{H}$ in the QP, originally defined as $\boldsymbol{H} \in \mathbb{R}^{2s\times 2s}$, is simplified here as $\boldsymbol{H} := \mathbf{I} \in \mathbb{R}^{s\times s}$.

In this reference case p^* is set to zero for each day of the month and the results give the lower theoretical bound on EC achievable by the scheduling algorithm. We denote this reference case as *RD* (reference daily).

4.3. Reference Algorithms

The CO-based scheduling algorithm is compared against two alternate approaches to designing day-ahead charge/discharge schedules. The two approaches, namely QP-based energy shifting and LP-based energy shifting have been presented in Ratnam et al. (2015a), and will serve as reference cases. Table 3 lists the objective function for each respective method. Each method is subject to the ESS constrains described in Section 2. We replicate the LP-based and QP-based methods in this paper for the purpose of benchmarking the proposed CO-based scheduling algorithm defined in Section 2.5.

LP: Best EC Minimization

The Linear Program maximizes the operational daily EC savings by energy shifting and/or energy arbitrage. When the customer cannot sell energy back to the grid, this method minimizes the operational costs by shifting energy use of the customer from on-peak pricing periods to off-peak pricing periods. When energy arbitrage is allowed, the net demand profile of the customer becomes irrelevant for ESS scheduling and the method instead focuses on maximizing the profit from arbitrage.

This method dispatches ESS in the most profitable way possible when the customer is not subject to a demand or a supply charge tariff. Thus it determines the upper performance bound for the EC minimization using ESS. We solve this optimization problem using MATLAB (Version 2016b) with the convex modeling framework CVX (Version 2.1) and the solver Gurobi (Version 7.0.2). We denote this reference method as *LP*.

QP: Mitigation of Power Fluctuations

The Quadratic Program minimizes the daily fluctuations in the net demand profile of the customer through energy shifting while also reducing peak net demand. It ignores the TOU rate structure. As a consequence, it does not necessarily improve the operational savings of the customer. This method depicts a grid-friendly ESS operation mode and represents the performance bound in that context. We solve this optimization problem using MATLAB's *interior-point-convex quadprog* algorithm. We denote this reference method as *QP*.

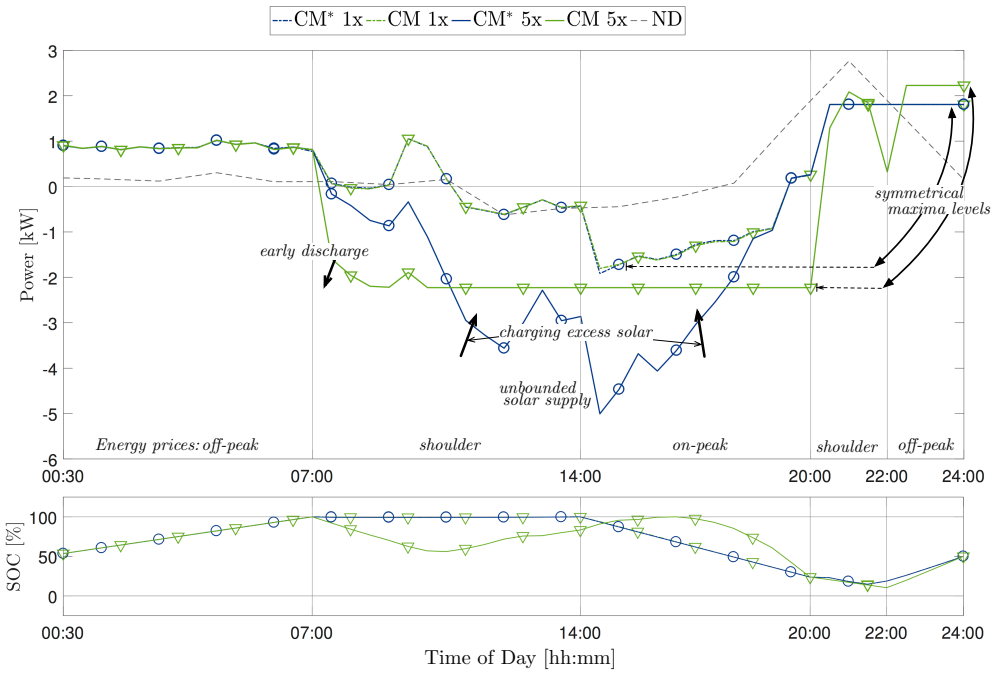

Figure 2: Scheduling under increasing solar PV penetration for the customer #38 with configuration d (with PV, exports allowed) on October 23, 2011. The customer net demand (with solar PV, but without ESS) is shown as ND and has a peak of 2.76 kW. Each case has a 30-minute resolution and 48 data points in total. To avoid cluttering, the lines are printed with sparser markers that are shown at different points in time. The original solar PV generation data (1x) has been increased by a factor of 5 (5x) to depict increasing PV penetration. The scheduling is done by applying only demand charge, *CM** (blue lines), and a capacity charge that includes a demand charge and a supply charge, *CM* (green lines) as in the rest of the paper.

4.4. Example CO-based algorithm schedule

An example charge schedule is given in Figure 2 for the *CM* (green lines) and the *CM** (blue lines). In this case the customer has a 1.05 kW solar PV system and can send back energy to the grid (configuration d). To demonstrate the characteristic behavior of the scheduling algorithm under increasing PV penetration, we increase the solar PV system size of the customer. We designate the customer with the original solar PV generation as 1x (dashed lines) and increase this generation by a factor of 5 (solid lines) denoted as 5x.

In all cases, the scheduling algorithm shifts customer load away from the on-peak pricing period and charges the ESS during the off-peak pricing periods while capping the net demand peak. Since the *CM** does not consider a supply charge tariff the solar generation is simply fed to the grid. The ESS is instead charged during the off-peak pricing period before 7:00 of the day until it is fully charged and then discharged during the on-peak pricing period to maximize cost reductions.

The *CM* follows the same scheduling in the 1x case with a single deviation in scheduling at 14:30 of the day when it restricts the maximum supply to the same level of the maximum demand to avoid an increase in the customer's peak capacity. We observe a significant change in scheduling pattern for the 5x case. The ESS is being discharged starting at 7:00 of the day in preparation for absorbing excess generation at solar peak hours and cap the maximum supply to the same level of the maximum demand. Nevertheless, the scheduling algorithm is still forced to increase the peak capacity of the customer by 23% in this case.

Table 4 shows how the maximum demand, the maximum supply, the energy cost to the customer and the PV self-consumption change with increased PV penetration levels. In addition to the cases in Figure 2, we also present results for the 2x case where the solar generation of the customer is increased by a factor of 2. The customer's energy cost is not impacted by the introduction of a supply charge in the 2x case and the ESS cycling does not change. The compensation to the customer is reduced roughly by 8% in the 5x case but the

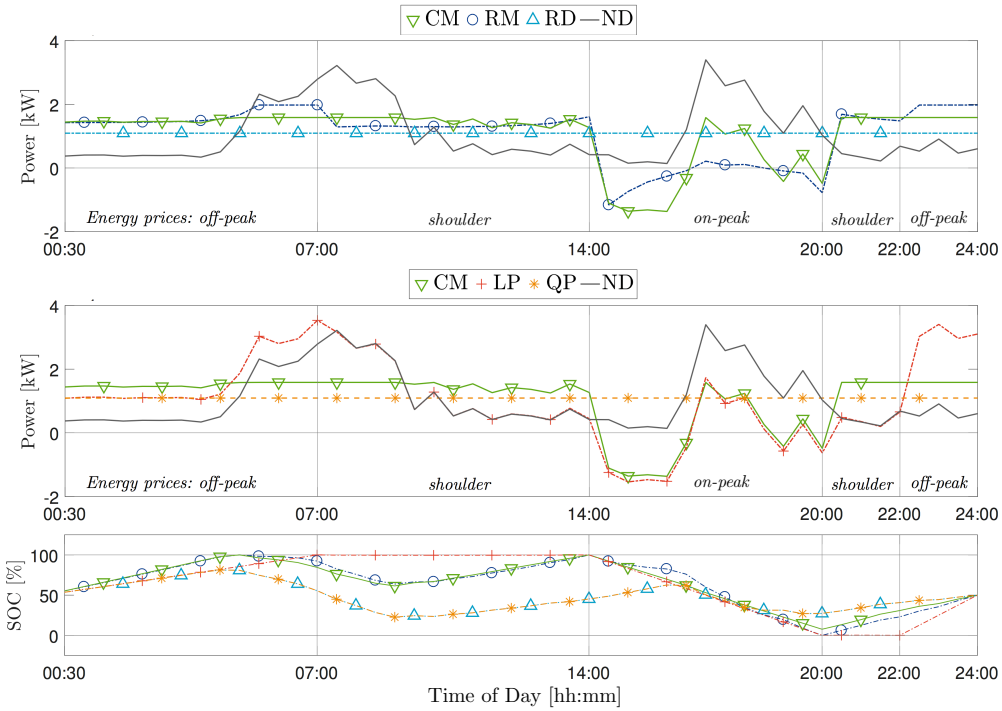

Figure 3: Comparison of the default case *CM* with the results from the reference cases *RM*, *RD* (top) and the reference algorithms *LP*, *QP* (middle) for customer #13 with configuration *b* (no PV, exports allowed) on May 15, 2012. The customer load has a peak of 3.40 kW and a minimum of 0.14 kW. The other cases have the following peak and minimum power in kW: *CM*: 1.59, -1.37; *RM*: 1.98, -1.16; *RD*: 1.09, 1.09; *QP*: 1.09, 1.09; *LP*: 3.53, -1.52. The acronyms here stand for *case monthly* (*CM*), *reference monthly* (*RM*), *reference daily* (*RD*), *linear program* (*LP*), *quadratic program* (*QP*), and *net demand* (*ND*).

customer's maximum energy supply is also significantly reduced from 3.73 kW to 2.23 kW. The ESS approximately makes one additional cycling for this case. The PV self-consumption stays similar for the 1x and 2x cases but it is increased by more than %14 with the introduction of a supply charge.

4.5. Example scheduling for all case studies

To present representative results for one day we consider the scenario where the customer can deliver energy back to the grid, and does not have a solar PV system (configuration *b*). The customer has an average daily load of 12.3 kWh with a minimum of 1.6 kWh and a maximum of 64.8 kWh. Figure 3 shows the net demand profiles and the SOC optimized under each case study excluding the *CM**. All charge schedules start the day with charging the ESS in the off-peak period. The *LP* case study shows energy being purchased and storage during the off-peak period until the ESS is full, and the ESS discharging during the peak period to maximize operational savings. The other case studies show the ESS being cycled during the day in order to reduce peak net demand. In all cases, the ESS charges after 22:00 to fulfill the SOC equality constraint at the end of the day.

There are three important observations in Figure 3: (1) The *RD* results in the same charge schedule as the *QP* even though the *QP* does not consider a TOU tariff in its formulation. The *RD* lacks a net demand prediction p^* and consequently it overvalues the peak reduction and flattens the net demand profile in the same way as the *QP*. (2) The *CM* reduces peak net demand to a greater degree than the *RM* for this particular day (see 06:00 - 07:00). However, when the billing month is considered this lower level of peak net demand is suboptimal with respect to the total monthly electric bill TC, for this particular customer. Since the *CM* does not have the same information as the *RM* it optimizes the scheduling for this day with a lower bound on peak net demand. Consequently, the *CM* looses flexibility associated with a higher bound on peak net demand which results in economically undesirable discharging during the off peak period (06:00

Table 4: Details of scheduling under increasing solar PV penetration for the customer #38 on October 23, 2011. Max. Supply is the maximum power that the customer supplies to the grid. Daily EC shows the daily energy cost of the customer. A negative value of Daily EC indicates a financial compensation to the customer. The values given in parentheses show results for the same customer without an ESS.

Demand Charge (CM)*	Max.	Max.	Daily	PV Self-	ESS
PV Penetration	Demand [kW]	Supply [kW]	EC [AU$]	consumption [%]	Cycling [#]
1x	1.81 (2.76)	1.92 (0.63)	-1.64 (0.60)	57.8 (49.8)	1.72
2x	1.81 (2.76)	2.67 (1.40)	-2.54 (0.60)	34.2 (31.1)	1.72
5x	1.81 (2.76)	5.01 (3.73)	-5.22 (0.60)	15.8 (14.9)	1.72
Capacity Charge (CM)	Max.	Max.	Daily	PV Self-	ESS
PV Penetration	Demand [kW]	Supply [kW]	EC [AU$]	consumption [%]	Cycling [#]
1x	1.81 (2.76)	1.81 (0.63)	-1.64 (0.60)	57.9 (49.8)	1.72
2x	1.81 (2.76)	1.81 (1.40)	-2.54 (0.60)	34.1 (31.1)	1.72
5x	2.23 (2.76)	2.23 (3.73)	-4.82 (0.60)	30.0 (14.9)	2.67

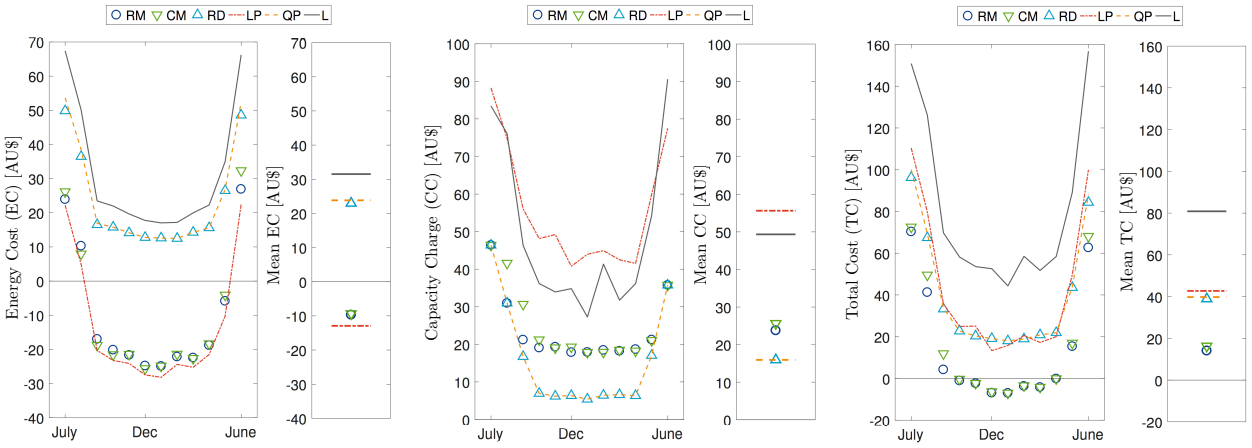

Figure 4: Electricity cost breakdown of all scheduling cases for the customer #13 with configuration *b* (no PV, exports allowed) covering a 2-year data set. The costs for the original customer load is shown as L. Scheduling is optimized during each billing month. The average (of the two) values for each billing month are shown. The annual mean for each case is shown to the right of each figure. Note that the June is Winter in the Southern hemisphere. The acronyms here stand for *case monthly* (*CM*), *reference monthly* (*RM*), *reference daily* (*RD*), *linear program* (*LP*), *quadratic program* (*QP*).

- 07:00). (3) The *LP* practically shifts the original peak net demand to the off-peak period without any mitigation of the peak net demand. It even causes a slight increase in peak net demand over the course of the day (by 4%).

In Figure 4, the electricity cost breakdown for the same scenario (customer #13 and configuration *b*) is shown for the 2-year data set. The *LP* marks the lowest bound on electricity charge EC, but the *RM* follows this bound very closely. This indicates that the CO-based scheduling algorithm results in charge schedules that perform near-optimally in EC reductions. Furthermore the *CM* yields similar results to the *RM* even without the same informational leverage that the *RM* has. This indicates that given an accurate daily load and solar forecast, and peak net demand predictions based on the previous month, the CO-based schedules can in fact yield near optimal EC reductions for customers in real world ESS operations. Lastly, capacity charges are minimized by the *QP* and *RD*, while the *LP* performs worst. For the total cost the *RM* and *CM* perform best.

4.6. Bulk Simulation Results

Using the Ausgrid data (Section 3.2) for each customer we perform the optimization with the case studies *CM*, *RM*, *RD*, *QP*, and *LP* for a 2-year period starting in July 2011. The last month of the first year has to be used for the net demand prediction for the first month of the second year in the *CM*. Therefore, we do not perform the optimization

for the first year in the context of the data set.

Figures 5 - 9 present the performance metric results for the bulk simulations. For each customer 24 metrics calculated for 24 billing months are averaged. The histograms show the distributions of the averaged value for 53 customers.

4.6.1. Electricity Cost

Figure 5 gives the electricity charge EC, the peak capacity charge CC, and the total monthly electricity bill TC for each customer system configuration. Overall the results are consistent with those observed for customer #13 in Figure 4, but they also highlight some differences between the configurations with and without grid exports. The *LP* yields greater reductions in EC in configurations *a* and *b*, where energy sale back to the grid is not incentivized. The *RM* and *CM* perform similarly to the *LP* with the performance especially close to the *LP* when energy arbitrage is allowed (configuration *b* and *d*). Scheduling through the *QP* results in the lowest CC (with RD a close second) since it focuses on flattening the net demand profile. The *RM* and *CM* also incur comparably small CC especially when energy sale back to the grid is not incentivized. These observations are in agreement with our earlier observations in Section 4.5.

4.6.2. Peak Reduction

Reducing peak demands generally goes along with reduced grid impacts as the infrastructure is utilized more evenly. Figure 6 shows peak reductions achieved by the *CM*, *QP*, and *LP*. For this figure and the following ones, we only report results for the *CM*, *QP*, and *LP* as the *RM* and *RD* do not show much difference from the *CM* and *QP*, respectively.

The *QP* results in the greatest reductions in peak net demand averaging 67 to 69%, depending on the configuration. The *CM* achieves comparable results in configurations *a* and *c* (61%, 64%, respectively) but in configuration *b* and *d* results in lesser peak net demand reductions (51%, 43%, respectively) in return for profit through energy arbitrage in the top row of Figure 5. The *LP* is ineffective in peak net demand mitigation and causes an increase in peak net demand for most customers.

4.6.3. Storage Cycling

Increased storage cycles go along with a reduction in ESS lifetime. The *QP* is the least straining on the ESS in terms of storage cycling in all configurations. For configuration *b*, the *CM* and *LP* cause a doubling in cycling due to energy arbitrage. In configuration *b* and *d* with grid exports allowed, the *LP* results in a single storage cycle per day for all customers and months; in these cases the *LP* profit is maximized by charging to 100% during the morning off-peak, discharging to 0% on-peak, and charging back up to 50% during the evening off-peak. Since the *CM* similarly utilizes only about one cycle per day in configurations b and d indicates that either (i) customer peak demands coincide with the on-peak period, so a discharging will accomplish both EC and CC objectives or (ii) the energy required to reduce peak demand is small compared to the ESS energy capacity. The cycling for the *CM* may increase compared to the *LP* if smaller batteries were considered.

4.6.4. Net Demand Fluctuation

Figure 8 shows fluctuations in net demand profiles for each configuration and without an ESS. The *QP* mostly achieves constant power (flat) customer net demand profiles and reduces net demand fluctuation dramatically. This indicates that the ESS is sized large in comparison to most customers' daily load variations. The *CM* results in 25 to 50% reductions in net demand fluctuations when compared to the original customer data, while the *LP* increases fluctuations by 13% for configuration *c* and yields reductions between 25 - 31% for others.

4.6.5. PV Self-Consumption

Figure 9 shows PV self-consumption for each configuration and without an ESS. All cases result in increased PV self-consumption when energy sale back is not incentivized. The *QP* overall results in the largest mean self-consumption with 89 - 93%. The *CM*, *QP*, and *LP* achieve the same mean self-consumption in configuration *c* with 93%, a substantial increase over 54% achieved without an ESS. When energy arbitrage is allowed the *CM* and *LP* yield lower self-consumptions but still 20% higher than the self-consumption without an ESS.

4.7. Impact of a Supply Charge on Solar Supply

In this paper we introduced a supply charge tariff that incentivizes ESS customers to store excess solar PV generation that would otherwise result in reverse power flow in the distribution grid. We compare the *CM* with the $CM^{\star}$ that does not consider a supply charge but still considers a demand charge.

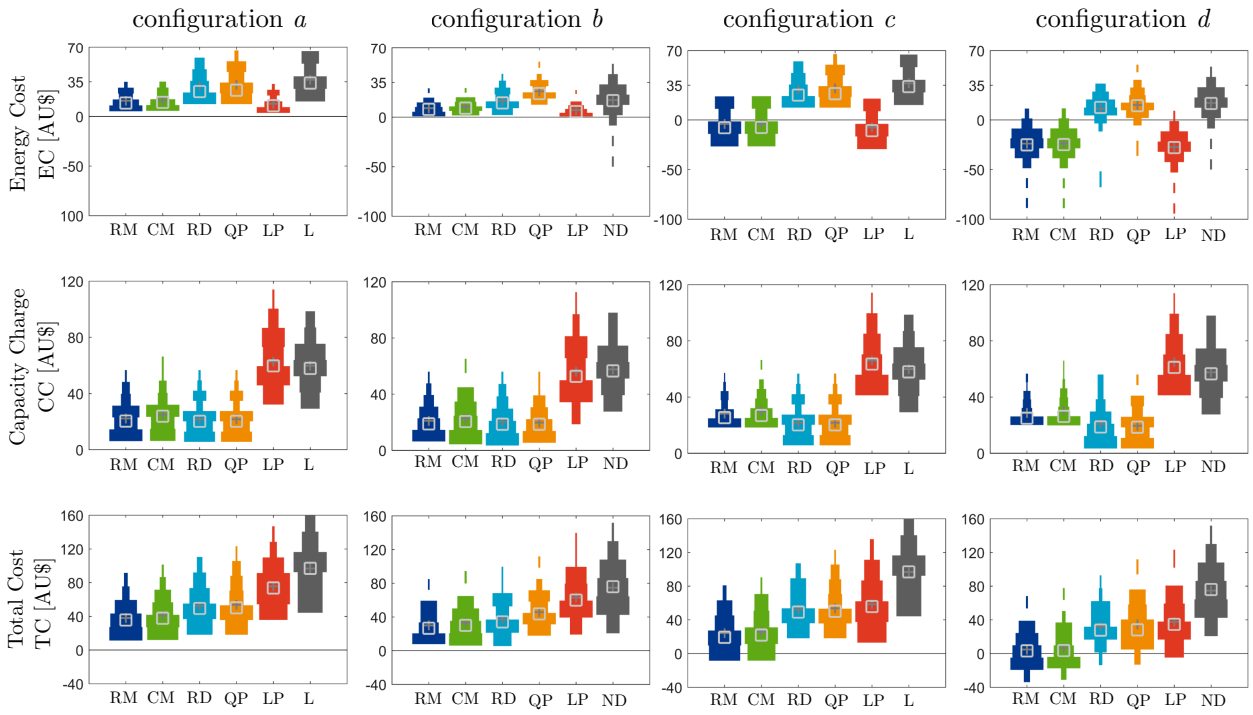

Figure 5: Electricity cost breakdown of all scheduling cases for 53 residential customers over a 2-year data set. The columns represent the different configurations given in Figure 1. The original customer data is labeled as L (load) when a solar PV system does not exist and labeled as ND (net demand) otherwise. 24 electricity cost values optimized for 24 billing months are averaged. Then a histogram is drawn for 53 customers. The variation in box plot thickness represents the distribution of the values. Thicker regions mean more customers fall in this bracket. A light colored square sign (□) indicates the median and a dark colored plus sign (+) shows the mean of all customers. A negative cost indicates compensation to the customer. The acronyms here stand for *case monthly* (CM), *reference monthly* (RM), *reference daily* (RD), *linear program* (LP), *quadratic program* (QP).

In order to compare performance of the CM and $CM^\star$, similar to the practice in Figure 2, we designate the customer with the original solar PV generation as 1x and increase this generation by a factor of 2. Here we only consider configuration d since configuration a and c do not have solar PV systems, and the constraint $\boldsymbol{p} \geq 0$ in configuration b avoids any energy to be supplied back to the grid, thus causes no difference in solar supply with increased PV penetration.

Figure 10 shows PV self-consumption, maximum supply to the grid, storage cycling and the total cost to the customer achieved in the CM and $CM^\star$. As the customers have larger solar PV systems the overall PV self-consumption decreases and the overall maximum supply to the grid increases in both cases. The maximum supply in Figure 10 reflects the capacity requirements of the infrastructure that would be required to support the PV system owners.

We observe that the CM yields higher PV self-consumption than the $CM^\star$ by 2% and 10% in the 1x case and the 2x case, respectively. Furthermore, it reduces the maximum reverse power flow to the grid in the 2x case by 0.60 kW on average from 4.2 kW without an ESS. The 1x case does not have enough solar PV feed-in (2.0 kW on average) to exceed the peak capacity of the customers and the maximum reverse power flow does not get penalized by a supply charge in most cases. It results in an increased ESS cycling by 3 cycles per month in the 2x case but causes approximately the same ESS cycling in the 1x case. Moreover, introduction of a supply charge has negligible impact on the customer TC. However, there are a few customers – presumably those with large PV systems – that need to cycle the ESS significantly more per month under the CM with up to 48 cycles. Presumably some of the same customers with the largest PV systems see their TC reimbursements from the utility cut sig-

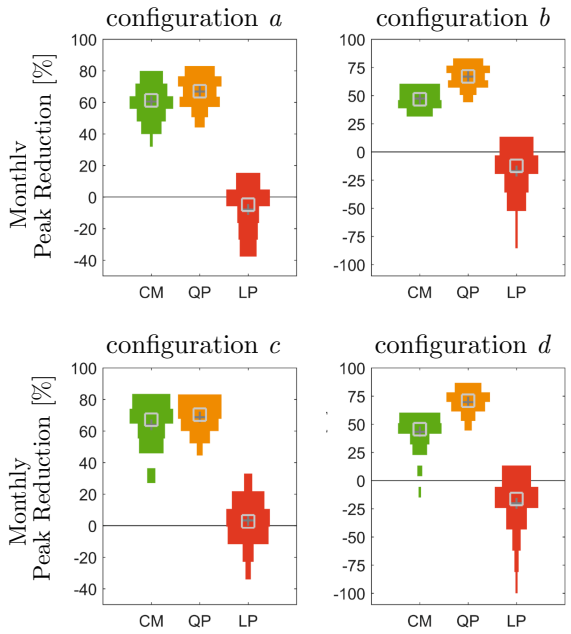

Figure 6: Monthly Peak Reductions achieved by the *CM*, *QP*, *LP* by configuration. Negative values indicate an increase in peak demand (primarily occurring for the *LP*).

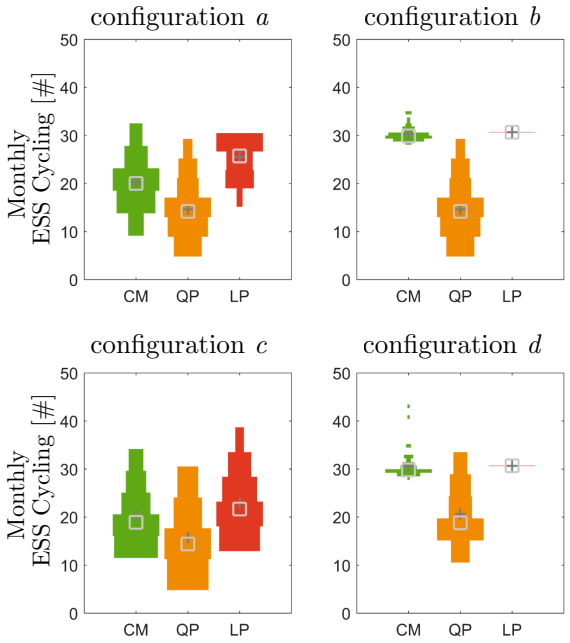

Figure 7: Monthly ESS cycling in the *CM*, *QP*, *LP* by configuration.

nificantly, from up to 140 AU$/month to less than 70 AU$/month.

5. Conclusions

We have presented a CO-based charge/discharge scheduling algorithm for distributed ESSs with co-located solar PV systems. The results of a case study including 53 residential customers located in an Australian distribution network confirmed that the daily CO-based charge/discharge schedules reduce (1) peak net demand of the customer (by design), (2) power fluctuations in the net demand profile (ancillary benefit), and (3) the reliance of the customer on the grid by way of promoting energy self-consumption of local solar PV generation (also an ancillary benefit).

We benchmark the performance of the CO-based scheduling algorithm with two alternate methods for behind-the-meter ESS scheduling. Results based on 2-years of customer data show that the CO-based scheduling algorithm provides mean monthly peak net demand reductions between 46% - 64%, reduces net demand fluctuations by 25% - 49% on average, and increases the mean solar PV self-consumption between 24% - 39% when compared to the original customer data. Maybe most importantly, the CO-based schedules yield a nearly optimal energy cost reductions.

Prior to deployment of this scheduling algorithm in real-world applications, further work is needed to show susceptibility of the algorithm to load and solar forecast accuracy as well as ESS sizing (specifically smaller ESS) and inclusion of ESS degradation costs. For specific applications the tariffs should obviously be adjusted to the local conditions.

In this paper we have also introduced the concept of having a supply charge in electricity rates. We demonstrated that the introduction of a supply charge does not financially impact customers with an ESS while it encourages customers to reduce their peak solar power supply to the grid. This new tariff mechanism reduces the maximum monthly solar PV power supply to the grid by 19% on average in the data set considered here.

We envision our assessment would assist policy makers in developing tariff structures where a penalty or subsidy on restricting solar power supply may encourage customers to reduce reverse power flow through procurement of an ESS. This, in return, would help utilities to support more distributed renewable energy generation on their distribution systems.

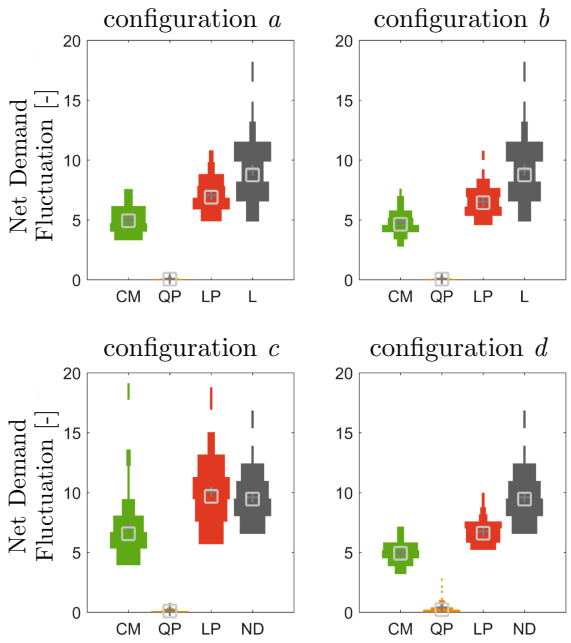

Figure 8: Net Demand Fluctuation for the *CM*, *QP*, *LP* by configuration in comparison with the original customer data (*L* or *ND*).

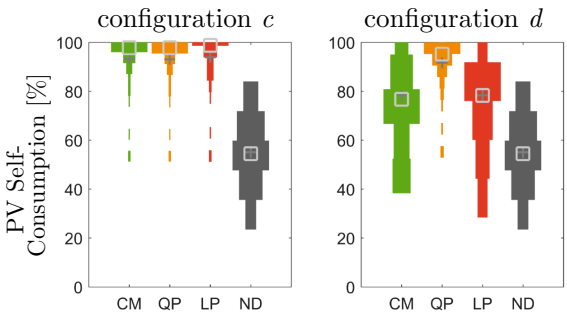

Figure 9: PV self-consumption achieved for the *CM*, *QP*, *LP* by configuration given along with direct PV self-consumption by the customer (*ND*) without an ESS.

6. Acknowledgements

The authors would like to thank Ryan Hanna for helpful comments and review.

References

Ausgrid, 2016. Price lists and policy: Network price list 2016 - 2017. [Online; accessed Feb. 2017.].
URL http://www.ausgrid.com.au/Common/Industry/Regulation/Network-prices/Price-lists-and-policy.aspx

Baran, M. E., Hooshyar, H., Shen, Z., Huang, A., Jun. 2012. Accommodating high PV penetration on distribution feeders. IEEE Transactions on Smart Grid 3 (2), 1039–1046.
URL http://dx.doi.org/10.1109/TSG.2012.2190759

Cutter, E., Haley, B., Hargreaves, J., Williams, J., Jul. 2014. Utility scale energy storage and the need for flexible capacity metrics. Applied Energy 124, 274–282.

de Sisternes, F. J., Jenkins, J. D., Botterud, A., Aug. 2016. The value of energy storage in decarbonizing the electricity sector. Applied Energy 175, 368–379.
URL https://doi.org/10.1016/2Fj.apenergy.2016.05.014

Denholm, P., Ela, E., Kirby, B., Milligan, M., Jan. 2010. The Role of Energy Storage with Renewable Electricity Generation. Tech. rep., National Renewable Energy Laboratory.
URL http://www.nrel.gov/docs/fy10osti/47187.pdf

DiOrio, N., Dobos, A., Janzou, S., Nov. 2015. Economic analysis case studies of battery energy storage with SAM. Tech. rep., National Renewable Energy Laboratory.
URL http://www.nrel.gov/docs/fy16osti/64987.pdf

Geem, Z. W., Yoon, Y., Mar. 2017. Harmony search optimization of renewable energy charging with energy storage system. International Journal of Electrical Power & Energy Systems 86, 120–126.
URL https://doi.org/10.1016/2Fj.ijepes.2016.04.028

Gitizadeh, M., Fakharzadegan, H., Feb. 2014. Battery capacity determination with respect to optimized energy dispatch schedule in grid-connected photovoltaic (PV) systems. Energy 65, 665–674.
URL https://doi.org/10.1016/2Fj.energy.2013.12.018

GP, 2016. Time of use - residential demand schedule. [Online; accessed Feb. 2017.].
URL https://www.georgiapower.com/docs/rates-schedules/residential-rates/2.40_TOU-RD.pdf

Hledik, R., Aug. 2014. Rediscovering residential demand charges. The Electricity Journal 27 (7), 82–96.
URL https://doi.org/10.1016/2Fj.tej.2014.07.003

Luthander, R., Widén, J., Munkhammar, J., Lingfors, D., Oct. 2016. Self-consumption enhancement and peak shaving of residential photovoltaics using storage and curtailment. Energy 112, 221–231.
URL https://doi.org/10.1016/2Fj.energy.2016.06.039

McLaren, J., Davidson, C., Miller, J., Bird, L., Oct. 2015. Impact of rate design alternatives on residential solar customer bills: Increased fixed charges, minimum bills and demand-based rates. The Electricity Journal 28 (8), 43–58.

Moshövel, J., Kairies, K.-P., Magnor, D., Leuthold, M., Bost, M., Gährs, S., Szczechowicz, E., Cramer, M., Sauer, D. U., Jan. 2015. Analysis of the maximal possible grid relief from PV-peak-power impacts by using storage systems for increased self-consumption. Applied Energy 137, 567–575.
URL https://doi.org/10.1016/2Fj.apenergy.2014.07.021

Ranaweera, I., Midtgård, O.-M., Apr. 2016. Optimization of operational cost for a grid-supporting PV system with battery storage. Renewable Energy 88, 262–272.
URL https://doi.org/10.1016/2Fj.renene.2015.11.044

Ratnam, E. L., Weller, S. R., Kellett, C. M., Mar. 2015a. An optimization-based approach to scheduling residential

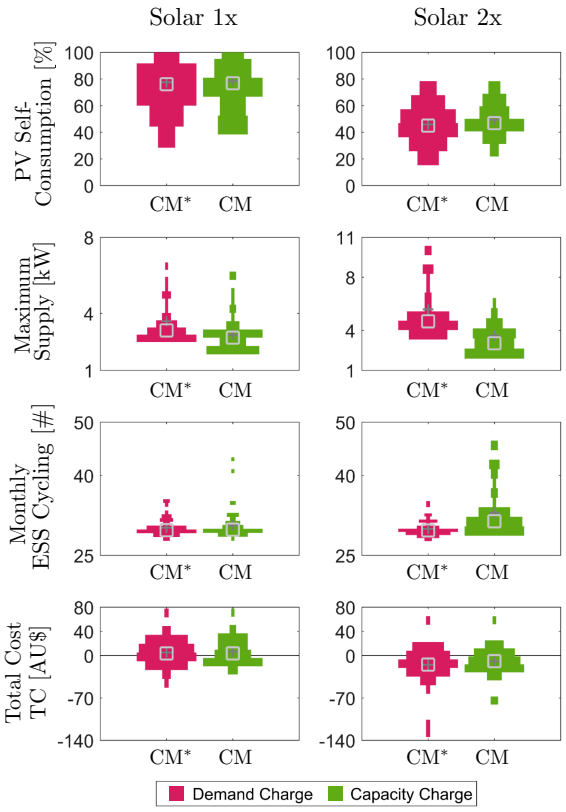

Figure 10: PV self-consumption, maximum solar supply to the grid, and total electricity cost under a capacity charge case (CM) and a demand charge only case ($CM^{\star}$). The original solar PV generation (1x) has been increased by a factor of 2 (2x) to investigate sensitivities. Maximum supply is determined by taking the highest amount of supply that the customer provided over the course of 2 years. A negative cost indicates compensation to the customer.

battery storage with solar PV: Assessing customer benefit. Renewable Energy 75, 123–134.
URL https://doi.org/10.1016/2Fj.renene.2014.09.008

Ratnam, E. L., Weller, S. R., Kellett, C. M., Murray, A. T., Oct. 2015b. Residential load and rooftop PV generation: an Australian distribution network dataset. International Journal of Sustainable Energy, 1–20.
URL https://doi.org/10.1080/2F14786451.2015.1100196

Ren, H., Wu, Q., Gao, W., Zhou, W., Oct. 2016a. Optimal operation of a grid-connected hybrid PV/fuel cell/battery energy system for residential applications. Energy 113, 702–712.
URL https://doi.org/10.1016/2Fj.energy.2016.07.091

Ren, Z., Grozev, G., Higgins, A., Apr. 2016b. Modelling impact of PV battery systems on energy consumption and bill savings of Australian houses under alternative tariff structures. Renewable Energy 89, 317–330.
URL https://doi.org/10.1016/2Fj.renene.2015.12.021

VEP, 2016. Schedule 1s residential service. [Online; accessed Feb. 2017.].
URL https://www.dom.com/library/domcom/pdfs/virginia-power/rates/residential-rates/schedule-1s.pdf

Vieira, F. M., Moura, P. S., de Almeida, A. T., Apr. 2017. Energy storage system for self-consumption of photovoltaic energy in residential zero energy buildings. Renewable Energy 103, 308–320.
URL https://doi.org/10.1016/2Fj.renene.2016.11.048

Zhang, Y., Lundblad, A., Campana, P. E., Yan, J., Jun. 2016. Employing battery storage to increase photovoltaic self-sufficiency in a residential building of Sweden. Energy Procedia 88, 455–461.
URL https://doi.org/10.1016/2Fj.egypro.2016.06.025

Zheng, M., Meinrenken, C. J., Lackner, K. S., Jun. 2015. Smart households: Dispatch strategies and economic analysis of distributed energy storage for residential peak shaving. Applied Energy 147, 246–257.
URL https://doi.org/10.1016/2Fj.apenergy.2015.02.039